Bonding Analysis of the $[C_2O_4]^{2+}$ Intermediate Formed in the Reaction of CO_2^{2+} with Neutral CO_2

Ferran Feixas,[†,‡] Robert Ponec,[*,†] Jiří Fišer,[§] Jana Roithová,[*,∥] Detlef Schröder,[⊥] and Stephen D. Price[#]

Institute of Process Fundamentals, Academy of Sciences of the Czech Republic, Rozvojová 135, 165 02, Prague 6, Suchdol 2, Czech Republic, Institute of Computational Chemistry and Department of Chemistry, University of Girona, Campus Montilivi, 17071 Girona, Spain, Department of Physical and Macromolecular Chemistry, Faculty of Sciences, Charles University in Prague, Hlavova 8, 12843 Prague 2, Czech Republic, Department of Organic and Nuclear Chemistry, Faculty of Sciences, Charles University in Prague, Hlavova 8, 12843 Prague 2, Czech Republic, Institute of Organic Chemistry and Biochemistry, Academy of Sciences of the Czech Republic, Flemingovo nám. 2, 166 10 Prague 6, Czech Republic, and Department of Chemistry, University College London, 20 Gordon Street, London WC1H 0AJ, United Kingdom

Received: March 7, 2010; Revised Manuscript Received: May 3, 2010

The bonding patterns of the $[C_2O_4]^{2+}$ dication formed upon interaction of CO_2^{2+} with neutral CO_2 are investigated using the analysis of domain-averaged Fermi holes (DAFHs). The DAFH approach provides an explanation for the previously observed "asymmetry" of the energy deposition in the pair of CO_2^+ monocations formed in the thermal reaction $CO_2^{2+} + CO_2 \rightarrow [C_2O_4]^{2+} \rightarrow 2\ CO_2^+$, specifically that the CO_2^+ monocation formed from the dication dissociates far more readily than the CO_2^+ monocation formed from the neutral molecule. The bonding pattern is consistent with a description of intermediate $[C_2O_4]^{2+}$ as a complex between the triplet ground state of CO_2^{2+} with the singlet ground state of neutral CO_2, which can, among other pathways, smoothly proceed to a nondegenerate pair of $^4CO_2^+ + {}^2CO_2^+$ where the former stems from the dication and the latter stems from the neutral reactant. Hence the "electronic history" of the components is retained in the $[C_2O_4]^{2+}$ intermediate. In addition, dissociation of $^4CO_2^+$ is discussed based on CCSD and CASSCF calculations. Equilibrium geometries for the ground electronic states of $CO_2^{0/+/2+}$ and some other relevant structures of CO_2^+ are determined using the MRCI method.

Introduction

Electron-transfer reactions between gaseous dications and neutral molecules have a long history in physical chemistry and chemical physics. Previous investigations of this topic led to the concept of the reaction-window theory, which states that electron transfer is kinetically most efficient if it occurs at an internuclear distance of about 2−6 Å, which roughly corresponds to the related exothermicities between 2−7 eV.[1,2] The reaction-window theory has been developed for collisions of atomic dications with neutral atoms, but several examples have demonstrated that it also holds true for (small) molecular dications.[2−4] In general, it is assumed that, in electron-transfer processes, the energy released upon the formation of two monocations from a dication and a neutral reagent is statistically partitioned between the resulting products, where most of the energy emerges as kinetic energy due to the Coulomb repulsion of the singly charged products. Recently, however, some of us have found indications that the internal energy partitioning can be nonstatistical in that the monocation originating from the dication dissociates substantially more than the monocation resulting from the neutral reaction partner.[5] These initial studies were, however, performed with organic hydrocarbon molecules, where, in addition to fundamental physical aspects of electron transfer, chemical phenomena (Franck−Condon effects, structural isomers, etc.) may also play a role and complicate the situation. To address this potentially asymmetric energy deposition in more detail, we have performed a series of detailed studies[6−10] of the reaction of the CO_2^{2+} dication with neutral CO_2, involving in some cases isotopic substitution. In addition to the potential relevance of the chemistry of CO_2^{2+} in the ionosphere of Mars,[11] these studies of $CO_2^{2+} + CO_2 \rightarrow 2\ CO_2^+$ are motivated by the fact that the geometries of CO_2 are very similar in all charge states involved in the electron transfer process (neutral, mono-, and dicationic);[12−15] indeed, even the anion radical $CO_2^{-\bullet}$ is not too different in geometry.[16] These experimental studies confirmed the occurrence of an apparently "asymmetric" energy deposition in that the amount of dissociation is significantly larger for the CO_2^+ monocation formed upon electron capture by the dication than for the CO_2^+ monocation generated by ionization of the neutral compound. This surprising behavior of the quasi-degenerate system of two CO_2^+ monocations has been attributed to the preferential formation of high-lying, predissociative quartet states upon electron capture by the triplet ground state of the dication, which are not accessible by a single-electron removal from the singlet ground state of neutral CO_2 (reaction 1, where the atoms of the dicationic reactant are highlighted in bold). The capture dication then dissociates rapidly according to reaction 2.[8]

* To whom correspondence should be addressed.
† Institute of Process Fundamentals, Academy of Sciences of the Czech Republic.
‡ University of Girona.
§ Department of Physical and Macromolecular Chemistry, Charles University in Prague.
∥ Department of Organic and Nuclear Chemistry, Charles University in Prague.
⊥ Institute of Organic Chemistry and Biochemistry, Academy of Sciences of the Czech Republic.
University College London.

10.1021/jp1020559
Published on Web 05/28/2010

$$CO_2^{2+}(^3\Sigma_g^-) + CO_2(^1\Sigma_g^+) \rightarrow CO_2^+(b^4\Pi_u) + CO_2^+(^2\Pi_g) \quad (1)$$

$$CO_2^+(b^4\Pi_u) \rightarrow CO^+(^2\Pi) + O(^3P) \quad (2)$$

A key feature of this collision system is its quasi-degeneracy: the two reagents have identical constituents, no isomers are involved, and neutral, singly charged, and doubly charged carbon dioxides have very similar geometries. Franck−Condon factors are therefore unlikely to play a role in differentiating the capture and ionization processes, and the singly charged products should be therefore formed with very similar vibrational energy distrubutions.

Position-sensitive coincidence (PSCO) experiments concerning the reaction $CO_2^{2+} + CO_2$ showed that the products of a nondissociative charge transfer emerge from an impulsive event without formation of an intermediate.[8] However, the PSCO signals from the dissociative charge transfer, forming CO^+ and O, reveal two components. The major part of the PSCO signal corresponds to the sequential dissociation of CO_2^+ formed in the impulsive event mentioned above, whereas the second part hints at the involvement of a long-lived intermediate $C_2O_4^{2+}$, which dissociates to $CO_2^+ + CO^+ + O$. This complex may dissociate to a pair of CO_2^+ monocations with one subsequently fragmenting to $CO^+ + O$, or the intermediate may first lose an oxygen atom to form $C_2O_3^{2+}$, which then fragments to $CO_2^+ + CO^+$. If the dissociation of the $C_2O_4^{2+}$ intermediate proceeds faster than any scrambling of atoms, and if the structure of this intermediate is asymmetric, it may result in the formation of $CO^+ + O$ from the original dication; this fragmentation would then offer an explanation for the experimentally observed asymmetry in charge transfer between CO_2^{2+} and CO_2. We note in passing that an analogous involvement of an intermediate in charge transfer and dissociative charge transfer has been recently shown for the reactions of the SiF_3^{2+} dication with N_2, CO, CO_2, O_2, and H_2.[17] Accordingly, a more detailed understanding of the bonding patterns of the transient intermediate $[C_2O_4]^{2+}$ may shed light on the energy distribution in this fundamental reaction. To this end, we report here an analysis of the $[C_2O_4]^{2+}$ intermediate formed from the reaction of the CO_2^{2+} in the ground states[18] and CO_2 using the analysis of domain-averaged Fermi holes (DAFHs) adopted for the treatment of open-shell molecules.[19] We note in passing that the excited states of CO_2^{2+} were shown to lead to a nondissociative electron transfer with CO_2, and therefore these states are not further considered to be involved in the reaction studied here.[20]

Methodology

The analysis of DAFHs was introduced some time ago as a new tool for the classification and elucidation of the nature of bonding interactions, especially in molecules with nontrivial bonding pattern such as multicenter bonding, hypervalence, metal−metal bonding, and so forth.[21−28] Despite valuable insight provided by this methodology, the applications of this approach have so far been restricted to systems with completely filled electron shells. This significant limitation has motivated us to extend the applicability of the DAFH approach to open-shell systems, such as those studied in this paper.

While the above generalization has recently been described,[19] the basic ideas of the proposed extension are briefly recalled to the extent necessary for this study. For this purpose, it is first useful to refer to the definition of DAFH for closed-shell systems. In this simple case, the Fermi hole averaged over the finite domain Ω is defined in eq 3.

$$g_\Omega(r_1) = N_\Omega \rho(r_1) - 2\int_\Omega \rho(r_1, r_2)\, dr_2 \quad (3)$$

where N_Ω denotes the number of electrons in the domain and $\rho(r_1)$ and $\rho(r_1,r_2)$ are the ordinary first-order electron density and electron-pair density, respectively. In the case of the Hartree−Fock (and formally also Kohn−Sham) approximation, the above formula reduces to eq 4:

$$g_\Omega(r_1) = 2\sum_i^{occ}\sum_j^{occ} \langle\phi_i|\phi_j\rangle_\Omega \phi_i(r_1)\phi_j(r_1) \quad (4)$$

where $\langle\phi_i|\phi_j\rangle_\Omega$ denotes the overlap integral of the molecular orbitals (MOs) ϕ_i and ϕ_j over the domain Ω as expressed in eq 5:

$$\langle\phi_i|\phi_j\rangle_\Omega = \int_\Omega \phi_i(r)\phi_j(r)\, dr \quad (5)$$

Although the holes can be generated and analyzed for domains of arbitrary size and shape, we have shown in previous studies that especially interesting and chemically relevant results can be obtained if the corresponding domains are identified with the atoms in molecules (AIM) atomic domains resulting from virial partitioning of the electron density.[29] In addition to the holes averaged over the domain of a single atom, the analysis can also be performed for more complex domains formed by combination of several atomic domains corresponding to specific molecular fragments (e.g., functional groups).

In view of the fact that the factor of 2 in eq 4 comes from the double occupancy of MOs in the wave function (Slater determinant) of the closed-shell systems, it is straightforward to assume that, in the case of unrestricted Hartree-Fock approximation, the formula (eq 4) can be rewritten as eq 6

$$g_\Omega(r_1) = \sum_i^{occ}\sum_j^{occ} \langle\varphi_i|\varphi_j\rangle_\Omega \varphi_i(r_1)\varphi_j(r_1) + \sum_i^{occ}\sum_j^{occ} \langle\psi_i|\psi_j\rangle_\Omega \psi_i(r_1)\psi_j(r_1) = g_\Omega^\alpha(r_1) + g_\Omega^\beta(r_1) \quad (6)$$

in which φ and ψ denote the (occupied) MOs for α and β spins, respectively. This equation suggests that, in the case of open-shell systems, the DAFHs are composed of two terms that can be regarded as the contributions of (domain averaged) Fermi holes of individual α and β spin electrons, respectively. This implies that in the case of open-shell systems, the DAFH analysis is to be performed for α and β spin electrons independently, and the resulting final picture of the bonding emerges from the superposition of the two complementary analyses. As the analysis of the holes corresponding to the electrons of the individual spins (α and β) is the same as in the case of closed-shell systems, we retain here only the specific differences arising from the open-shell nature of the approach. The first step of the analysis involves the diagonalization of the matrices representing the hole for each particular spin on the basis of MOs φ and ψ, respectively. The eigenvalues and eigenvectors generated in this primary diagonalization are then subjected to the so-called isopycnic transformation,[30] which

SCHEME 1: B3LYP/6-311G* Optimized Structure of the $[C_2O_4]^{2+}$ Intermediate with Notation of the Six Atoms Involved, Where O(1)C(2)O(3) Stems from the Neutral CO_2 Molecule and O(5)C(4)O(6) Stems from the Dicationic Reactant CO_2^{2+}

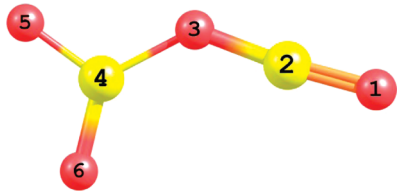

converts the original delocalized eigenvectors into more localized functions. The inspection of these localized orbitals straightforwardly allows one to identify the localized shared electron pairs corresponding to chemical bonds, lone pairs, and so forth, as well as the nature and the localization of unpaired electrons in the molecule.

Computational Details

In order to reveal the possible origin of the experimentally observed asymmetry of the energy decomposition in the pair of CO_2^+ monocations formed in the reaction of $CO_2^{2+} + CO_2$ as well as to evaluate the role in this reaction of the presumed intermediate $[C_2O_4]^{2+}$, we report in this study the following:

(1) The detailed analysis of the picture of the bonding in the above intermediate using the methodology of DAFH analysis. These calculations have been performed for the holes generated from the wave functions calculated at the UB3LYP/6-311G* level of theory for the previously optimized geometry of the studied dication.[7] In this connection it is fair to say that the level of the theory used for the DAFH analysis in this study is lower than the one used for the geometry optimization, but its choice was dictated by the fact that the application of the above analysis at the post-Hartree−Fock level of the theory requires knowledge of the correlated pair densities whose extraction from existing quantum chemical programs is not an easy task and, although first examples of such such an "exact" DAFH approach were recently reported,[31] its use for the present systems is beyond the scope of our possibilities. The DAFH analysis was performed using our program WinBaderO, which is available upon request. This program requires as input two files. One of them is the ordinary output file of the Gaussian 03 program[32] generated using appropriate keywords; the other is the file resulting from the Bader AIM analysis of the wfn files of the corresponding species and providing the so-called AOM matrices required for the DAFH analysis at the level of the exact AIM-generalized approach (see eq 6). These calculations were performed using the program AIMAll.[33] In addition, the traditional AIM analysis performed using the same program detected the existence of bond paths and bond critical points consistent with the bonding topology of the dication (Scheme 2).

(2) The detailed analysis of fate of the excited states of CO_2^+ formed by the dissociation of the transient $[C_2O_4]^{2+}$ intermediate involving the theoretical description of the energetics and dissociation pathways of the quartet states of CO_2^+. The geometry optimization was performed at the CCSD/cc-pVTZ[34,35] level of theory as implemented in the Gaussian 03 suite.[32] For all optimized structures, frequency analysis at the same level of theory was performed in order to assign them as genuine minima. The electronic structure calculations were performed using the complete active space self-consistent field (CASSCF)[36]

SCHEME 2: Bond Paths and Bond Critical Points Detected in the Traditional AIM Analysis of the Triplet State of Dication $[C_2O_4]^{2+}$

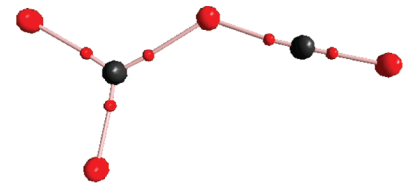

and the internally contracted multireference configuration interaction (MRCI)[37,38] method. The full valence active space (15 electrons in 12 orbitals) was used. The core MOs were constrained to double occupation but fully optimized. The correlation-consistent cc-pVQZ basis set of Dunning[35] was employed. The CASSCF and MRCI calculations were performed using the MOLPRO2006.1 suite of programs.[39]

Results and Discussion

After having introduced the basic ideas of the generalization of the DAFH approach to open-shell systems, we now discuss the picture of the bonding that emerges from the DAFH analysis of the triplet state of $[C_2O_4]^{2+}$. We also consider the potential role of this species as an intermediate in the $CO_2^{2+} + CO_2 \rightarrow 2\ CO_2^+$ reaction and how the intermediate may be involved in the observed "asymmetry" of the energy deposition in the pair of CO_2^+ product monocations. The formation of the transient intermediates $[C_2O_4]^{2+}$ in the $CO_2^{2+} + CO_2$ reaction was investigated before, and the structure considered here is the most stable isomer in the triplet state, and is thus formed from the ground states of both reactants. It was also shown that chemistry of this intermediate explains the formation of the experimentally observed bond-forming product $C_2O_3^{2+}$.[7]

The energetic asymmetry in the electron transfer between CO_2^{2+} and CO_2 discussed above is potentially linked to the formation of the quartet state ($b^4\Pi_u$) of the CO_2^+ product of electron capture; the natural choice for the DAFH analysis is the holes averaged over the fragments O(5)C(4)O(6) and O(1)C(2)O(3), respectively, where we use the notation of the atoms shown in Scheme 1. The analysis was performed for the holes generated from the wave function calculated for the completely optimized molecular geometry of the studied dication at the UB3LYP/6-311G* level of theory.[7]

We start with the DAFH analysis for the holes averaged over the fragment O(5)C(4)O(6) of $[C_2O_4]^{2+}$, which are summarized in Table 1. Consistent with the triplet nature of the dication, the DAFH analysis detects the existence of 12 nonzero eigenvalues for the electrons of α-spin and 10 nonzero eigenvalues for the electrons of β-spin. In order to understand the implications of this result for the bonding in the O(5)C(4)O(6) fragment, it is useful to examine the numerical data in Table 1 together with the graphical representations of the associated localized functions in Figures 1 and 2. The inspection of the eigenfunctions summarized in Figure 1 shows that the form of these localized functions is very similar for electrons of both α- and β-spin. This similarity, together with the corresponding eigenvalues lying close to unity (Table 1), clearly indicates these localized functions are associated with electron pairs (chemical bonds and/or core or lone electron pairs) involving two electrons of opposite spin. This is, for example, the case of the $1s^2$ core pair on the central carbon C(4) (Figure 1a,f), the σ-lone pair on the oxygen O(5) (Figure 1b,g), the electron pairs of σ_{CO} bonds (Figure 1c,d versus h,i, respectively). The remaining localized

TABLE 1: Eigenvalues of the DAFH and Their Assignments of the α- and *β*-Spin Electrons in the Fragment O(5)C(4)O(6) of the Triplet State of the Transient Complex $[C_2O_4]^{2+}$

eigenvalue		
α-spin	*β*-spin	assignment
1.000	1.000	$1s^2$ {O(5)}
1.000	1.000	$1s^2$ {O(6)}
1.000	1.000	$1s^2$ {C(4)} (Figure 1a,f)
1.000	1.000	*σ* {O(5)} (Figure 1b,g)
1.000	1.000	*σ* {O(6)}
0.989	0.984	*σ* {C(4)O(5)} (Figure 1c,h)
0.992	0.988	*σ* {C(4)O(6)} (Figure 1d,i)
0.207	0.204	Broken valence *σ* {C(4)O(3)} (Figure 1e,j)
0.992	0.989	see Figure 2
0.993		see Figure 2
0.994	0.977	see Figure 2
0.993		see Figure 2

α and *β* functions (Figures 1e,j) also have very similar shapes, typical of those for a shared electron pair. Obviously, this electron pair is partly localized in the O(5)C(4)O(6) fragment and partly in the O(1)C(2)O(3) fragment, and such localized functions with eigenvalues deviating significantly from unity correspond to so-called *broken valences*. Equal sharing of an electron pair between two fragments would be associated with eigenvalues of about 0.5 for a function localized on a given fragment. The eigenvalues of about 0.2 determined here suggest an uneven splitting of the electron pair between the fragments, which thus corresponds to a polar bond. The localized functions (Figure 1e,j) can be thus regarded as corresponding to a broken valence of the bond C(4)O(3), and the total population (0.207 + 0.204) can be then regarded as the contribution of carbon C(4) to the unevenly shared electron pair between C(4) and O(3). The remaining roughly 1.6 electrons required to complement the unevenly shared electron pair of the polar C(4) O(3) bond can be detected in the DAFH analysis of the hole averaged over the complementary O(1)C(2)O(3) fragment (see Table 2).

In order to complete the picture of the bonding in the O(5)C(4)O(6) fragment, it is now necessary to take into account the remaining group of DAFH eigenvectors summarized in Figure 2 (and the associated eigenvalues included in Table 1). The most important conclusion derived from Figure 2 is the lack of the ideal pairing of DAFH eigenvectors corresponding to α- and *β*-spin electrons. This lack of pairing is manifested not only in the different forms of DAFH eigenvectors corresponding to α- and *β*-spin electrons, but also in the significant difference between the number of these eigenvectors and their associated eigenvalues. These differences are evidently associated with the open-shell character of $[C_2O_4]^{2+}$. The fact that the number of α-spin eigenvalues exceeds the number of *β*-spin eigenvalues by two thus clearly indicates that the local electron structure of the fragment within the whole complex is close to that of a triplet.

The "local triplet state" of the O(5)C(4)O(6) fragment revealed by our calculations provides additional arguments in favor of the proposed role of the complex $[C_2O_4]^{2+}$ in the reaction of CO_2^{2+} with CO_2. A closer inspection of the forms and the symmetries of the DAFH eigenvectors in Figure 2 reveals a fundamental splitting of the DAFH eigenvectors into two groups, one of which is localized in the molecular plane, and the other is perpendicular to it, with dramatic differences between eigenvectors associated with α- and *β*-spin, respectively (for a more detailed discussion, see the Appendix). The DAFH eigenvectors associated with α spin in Figure 2 correspond to four electrons localized at O(5) (a), O(6) (b), *σ*(C(4)O(5)) (c), and *σ*(C(4)O(6)) (d), respectively. Instead of four complementary DAFH eigenvectors associated with *β*-spin electrons, only two eigenvectors are found. The first *β*-spin DAFH (e) is delocalized over both oxygen atoms and can be viewed as corresponding to an electron paired with an α electron in DAFHs a or b. The second *β*-spin DAFH (f) is delocalized over the whole fragment O(5)C(4)O(6) with a *π*-symmetry and corresponds to an electron to be paired with an α electron in DAFHs c or d. Hence, the unpaired α electrons reside in the *π*-bonding orbital delocalized over O(5)C(4)O(6) and in the nonbonding orbital delocalized between O(5) and O(6).

The existence of two unpaired electrons within the fragment O(5)C(4)O(6) of the intermediate complex $[C_2O_4]^{2+}$, which originates from the dication CO_2^{2+}, clearly implies that no unpaired electrons should be expected in the complementary fragment O(1)C(2)O(3), and its local electron structure should thus be close to that of a singlet. This expectation is indeed confirmed by the existence of strict pairing between the α- and *β*-spin eigenvectors and eigenvalues of the corresponding DAFH (Table 2). On the basis of the above analysis of the DAFHs, we deduce that O(1) and C(2) are bonded by a triple bond, and O(1) bears a nonbonding electron pair, whereas O(3) is bound to C(2) only by a single *σ*-bond, bears two nonbonding electron pairs, and has one broken valence pointing toward C(4). The shape of the α- and *β*-spin eigenvectors corresponding to this broken valence is very reminiscent of the complementary eigenvectors (Figure 1e,f) from the analysis of the hole averaged over the fragment O(3)C(4)O(5), and their populations closely agree with the expectations (Table 2).

In summary, the DAFH analysis averaged over the complementary fragments O(5)C(4)O(6) and O(1)C(2)O(3) provides a comprehensive picture of the bonding in the $[C_2O_4]^{2+}$ intermediate, which can be simply depicted in terms of resonant structures in Scheme 3. The O(1)C(2)O(3) has a closed-shell configuration and is bound to the O(5)C(4)O(6) fragment by a polar σ_{CO} bond.

The existence of a transient $[C_2O_4]^{2+}$ species can provide a simple rationale for the mechanism of electron reorganization in electron transfer between CO_2 and CO_2^{2+} (reaction 1). Splitting of the polar σ_{CO} bond between O(3) and C(4) is associated with the formation of singly charged $O(1)C(2)O(3)^+$ with the electron being removed from the nonbonding electron pair localized at oxygen. This process accordingly leads to the formation of CO_2^+ in the ground electronic state. The remaining singly charged ion, $O(5)C(4)O(6)^+$, bears three unpaired electrons and corresponds therefore to a quartet state. Notably, due to the asymmetry of the $[C_2O_4]^{2+}$ intermediate, the unpaired electron density stays localized at the fragment originally coming from the doubly charged reactant CO_2^{2+}. The involvement of a transient $[C_2O_4]^{2+}$ intermediate in this electron-transfer reaction can thus account for the different behavior of the capture and ionization monocations observed in the experiments. As an approximate first estimate, one might expect that the dynamical influence of such an intermediate may be significant for collisions with energies below or on the order of the relative binding energy of the intermediates with respect to the reactant asymptote. For the $[C_2O_4]^{2+}$ species, where we have previously calculated a relative binding energy of 4.5 eV,[7] this indicates that collisions for dications with energies up to approximately 8 eV in the laboratory frame may be influenced by the decay of this transitory species. The electronic effect of complexation should enhance the electronic effects in the direct electron-

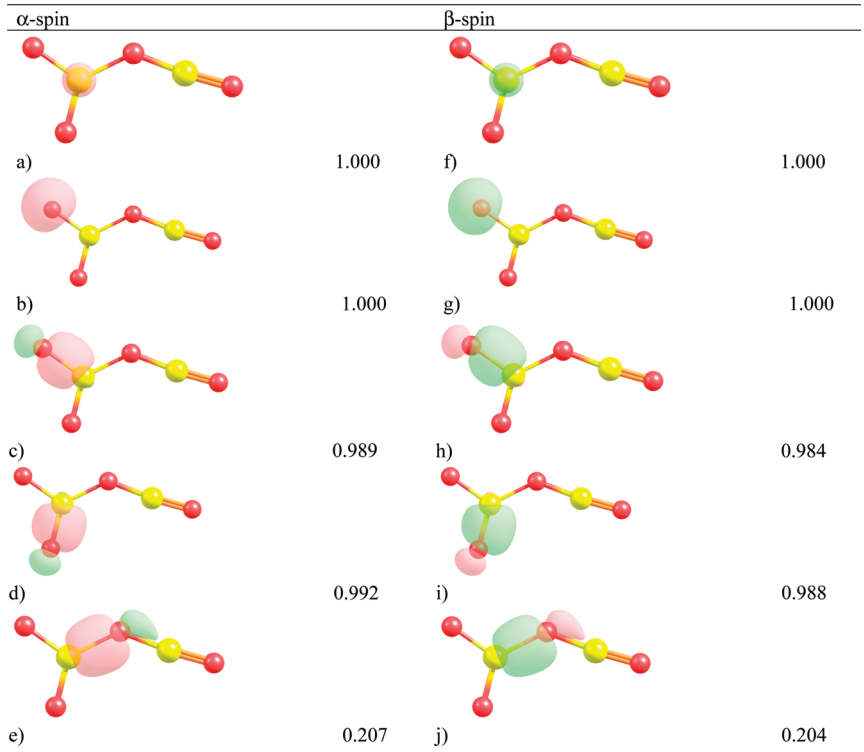

Figure 1. Selected eigenvectors of the DAFH corresponding to completely paired α- and *β*-spin electrons in the fragment O(5)C(4)O(6) of the triplet state of the transient complex $[C_2O_4]^{2+}$.

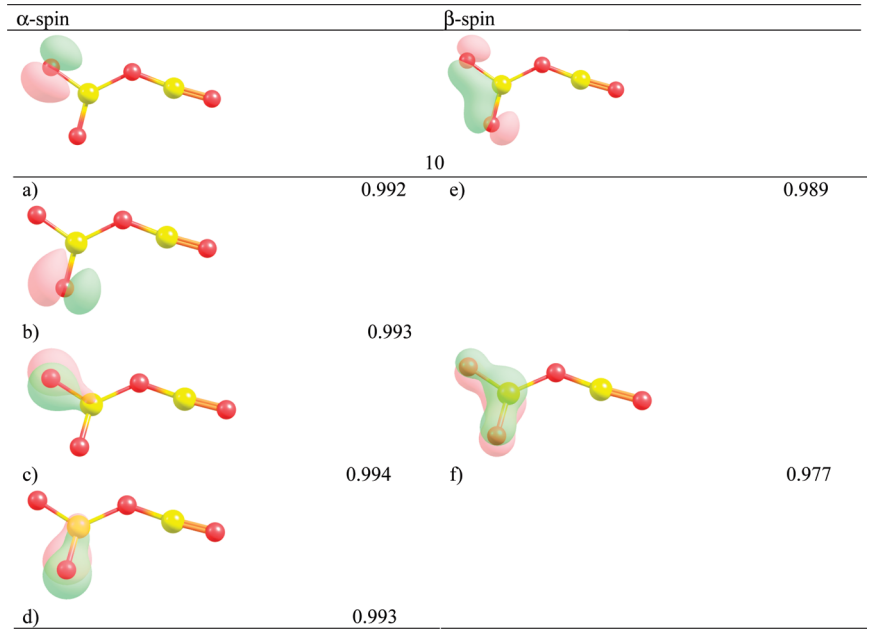

Figure 2. Selected eigenvectors of the DAFH responsible for the open-shell character in the fragment O(5)C(4)O(6) of the triplet state of the transient complex $[C_2O_4]^{2+}$.

transfer process, which also favor preferential decay of the CO_2^+ ions formed from the dication.[8]

Finally, we address the fate of the quartet CO_2^+ formed in the dissociation of the transient $[C_2O_4]^{2+}$ intermediate. All previous theoretical studies considered only linear geometries of the excited states of CO_2^+. Two quartet states lying lowest in energy correspond to $a^4\Sigma_g$ and $b^4\Pi_u$ symmetries.[40] Our previous preliminary B3LYP calculations revealed, however, that the geometry of the excited quartet state is not linear in that the bending of the cation leads to the stabilization of this quartet state by more than 4 eV.[10] In order to unravel the structures of the quartet states and to provide an explanation of the fragmentation of the CO_2^+ cation formed from dissociation of $[C_2O_4]^{2+}$, we have performed CCSD/cc-pVTZ calculations of the potential-energy profiles along the dissociation coordinates of the lowest quartet states, complemented by a benchmark *ab initio* investigation of the geometries as well as of the potential-energy surface associated with dissociation of the quartet states of CO_2^+.

The CCSD calculations reveal that the lowest-lying quartet state of CO_2^+ has a bent geometry with C_{2v} symmetry (R_{CO} = 1.263, α = 107.8°), which corresponds to the $^4B_1$ state ($^4A''$ in

TABLE 2: Eigenvalues of the DAFH and Their Assignments of the α- and β-Spin Electrons in the Fragment O(1)C(2)O(3) of the Triplet State of Transient Complex $[C_2O_4]^{2+}$

eigenvalue		
α-spin	β-spin	assignment
1.000	1.000	$1s^2$ {O(1)}
1.000	1.000	$1s^2$ {O(3)}
1.000	1.000	$1s^2$ {C(2)}
1.000	1.000	σ {O(1)}
0.999	0.999	σ {C(2)O(1)}
0.990	0.987	σ {C(2)O(3)}
0.988	0.984	σ {O(3)} in plane
0.996	0.997	π {C(2)O(1)} in plane
0.997	0.996	π {C(2)O(1)} perpendicular
0.943	0.960	σ {O(3)} perpendicular
0.798	0.802	broken valence σ {C(4)O(3)}

SCHEME 3

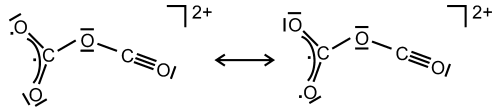

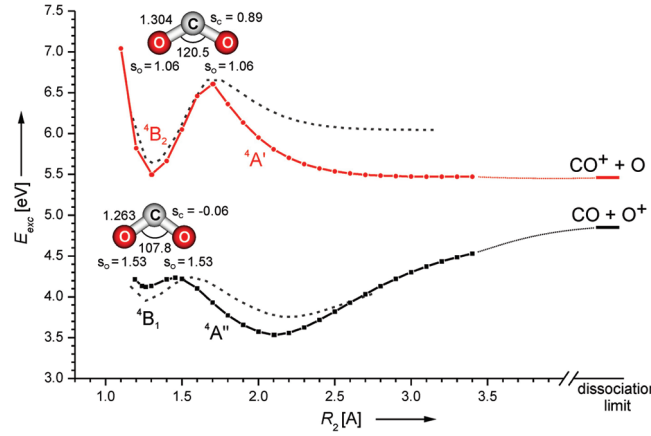

Figure 3. CCSD/cc-pVTZ PECs along the elongation of the C−O bond of the $^4A'$ and $^4A''$ states of CO_2^+. While one of the C−O bond is gradually elongated (R_2), the other C−O bond as well as the angle are optimized. The structures represent the covalent minima along the PECs and the numbers give optimized geometry parameters in angstroms and degrees. The values denoted s_X show the spin densities at the atom X determined by the Mulliken population analysis. The gray dashed lines give the analogous curves calculated at the B3LYP/6-311+G(2d,p) level of theory.

C_s symmetry) and lies 4.12 eV above the doublet ground state ($X^2\Pi_g$). The optimization of the second excited quartet state leads to a $^4B_2$ state ($^4A'$ in C_s symmetry), which bears again C_{2v} symmetry (R_{CO} = 1.304, α = 120.5°) and lies 5.50 eV above the CO_2^+ ground state. The benchmark MRCI calculations confirm these results (Table 3) and provide very similar geometries for both quartet states. The excitation energies are slightly shifted to 4.19 eV for the $^4B_1$ ($^4A''$) state and to 5.80 eV for the $^4B_2$ ($^4A'$) state. For both quartet states, additional minima on the potential-energy surface were localized, which correspond to predissociative complexes of CO with O^+ ($^4A''$ state) and CO^+ with O ($^4A'$ state), respectively. These minima are lower in energy than the covalent structures (Table 3). While the latter complex ($^4A'$ state) retains the bent geometry, the optimized structure of the former complex has a linear geometry. Detailed analysis reveals that the $^4B_1$ ($^4A''$) state correlates with the dissociation limit $O^+(^4S_u)$ + $CO(X^1\Sigma^+)$, whereas the $^4B_2$ ($^4A'$) state correlates with $O(^3P_g)$ + $CO^+(X^2\Sigma^+)$. Table 3 also includes the vertical excitation energies of the CO_2^+ dication ($X^2\Pi_g$) to the various quartet states. The enormous energy differences between the vertical and adiabatic excitation energies (6.13 eV for the $^4B_1$ state and 2.56 eV for the $^4B_2$ state) are predominately caused by the bending of the quartet states of CO_2^+ and show the importance of the inclusion of these geometrical changes in the theoretical investigations.

The results of our computational investigation of the dissociation of the quartet states of CO_2^+, at the CCSD level, are presented in Figure 3. The potential-energy curves (PECs) along the elongation of the C−O bond show that the covalent structures of both quartet states are separated from the predissociative complexes by a small energy barrier. The barriers amount to 0.1 eV for the $^4A''$ ($^4B_1$) state and 1.1 eV for the $^4A'$ ($^4B_2$) state. The insets in Figure 3 show the optimized covalent structures and the spin densities at each atom as determined by Mulliken population analysis. The three unpaired electrons are localized only at the oxygen atoms in the $^4B_1$ state, whereas each atom bears one unpaired electron in the $^4B_2$ state. The CO_2^+ cation formed by the electron capture in the CO_2^{2+} + CO_2 reaction proceeding via the $[C_2O_4]^{2+}$ intermediate bears also an unpaired electron at the carbon atom. The theoretical results thus predict that the electron transfer triggered by the formation

TABLE 3: Energetical and Geometrical Characteristics of Some Relevant States of $CO_2^{0/+/2+}$ Calculated at the MRCI/vqz Level

			geometry				
species	state linear geometry	state bent geometry	R_1/Å	R_2/Å	α/degree	energy/eV[a]	origin of the state
CO_2	$X^1\Sigma_g^+$		1.1622	1.1622	180	−13.47	
CO_2^+	$X^2\Pi_g$		1.1764	1.1764	180	0.0	
	$a^4\Sigma_g^-$	$^4B_1$ ($^4A''$)	1.268	1.268	108.6	4.19	local minimum[c]
	$a^4\Sigma_g^-$		1.119	2.046	180	3.92	global minimum[e]
	$a^4\Sigma_g^-$		1.1764	1.1764	180	10.32	vertical excitation
	$a^4\Sigma_g^-$		1.132	100	(180)	5.22	$O^+(^4S_u)$+$CO(X^1\Sigma^+)$[f]
	$b^4\Pi_u$	$^4B_2$ ($^4A'$)	1.308	1.308	120.1	5.80	local minimum
	$b^4\Pi_u$	$^4B_2$ ($^4A'$)	1.122	2.484	103.4	5.74	2. local minimum[d]
	$b^4\Pi_u$		1.1764	1.1764	180	8.36	vertical excitation[b]
	$b^4\Pi_u$		1.118	100	(180)	5.64	$O(^3P_g)$ + $CO^+(X^2\Sigma^+)$[f]
	$c^4\Pi_g$	2^4B_2 ($2^4A'$)	1.333	1.333	127.2	7.17	local minimum
	$c^4\Pi_g$		1.1764	1.1764	180	9.48	vertical excitation
CO_2^{2+}	$X^3\Sigma_g^-$		1.2140	1.2140	180	23.29	
	$X^3\Sigma_g^-$		1.1764	1.1764	180	23.40	vertical ionization[b]

[a] Energies are related to the ground electronic state of $CO_2^+(X^2\Pi_g)$ with E_{el} = −187.846683 hartree. [b] From the state $CO_2^+(X^2\Pi_g)$. [c] In the range of R_1, R_2 < 1.5 Å. [d] In the range of R_1< 1.5 Å, R_2 > 1.5 Å. [e] For a given spin state. [f] Dissociation limit.

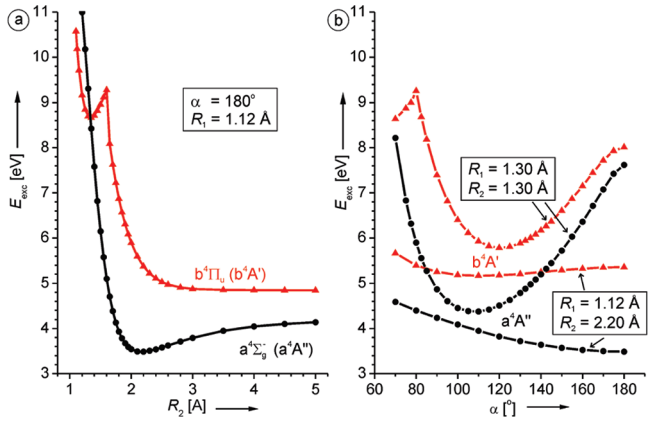

Figure 4. CASSCF PECs of the two lowest quartet states of CO_2^+, which are given with respect to the potential-energy minimum of the ground state of $CO_2^+(X^2\Pi_g)$. D_{2h} and C_s geometries were used as a reference. (a) PEC along R_2(CO) with R_1(CO) = 1.12 Å and α(OCO) = 180°. (b) PEC along α(OCO) with R_1(CO) = 1.12 Å and R_2(CO) = 2.20 and R_1(CO) = R_2(CO) = 1.30 Å, respectively, as specified in the figure.

of the $[C_2O_4]^{2+}$ intermediate should lead to the $^4B_2$ state of CO_2^+ formed from the dication, which should further dissociate into $CO^+ + O$. This theoretical deduction is exactly in line with what is observed in the experiment.[8]

We note in passing that the energetically lowest dissociation pathways calculated at the B3LYP/6-311+G(2d,p) level of theory (given as gray dashed lines in Figure 3) agree quite well with the CCSD results at the range of covalent minima. The agreement is less satisfactory at larger CO internuclear distances. The description of the dissociation behavior of the excited quartet states is, however, even at the B3LYP level, qualitatively correct.

As a final test, we probed the above predictions by benchmark CASSCF calculations of one-dimensional cuts of the potential-energy surfaces of the two lowest quartet states of CO_2^+. Figure 4 shows the PECs along the dissociation of the CO bond the O−C−O angle frozen at 180° and the other CO bond at 1.12 Å; energy is given relative to the energy of the equilibrium geometry of $CO_2^+(X^2\Pi_g)$. These curves reproduce well the curves published by Liu et al.[40] However, as mentioned above, the consideration of bending is essential for correct description of the quartet states. Figure 4b shows the effect of bending with geometries of R_1(CO) = 1.12 Å and R_2(CO) = 2.20 Å (the minimum localized for the $a^4\Sigma_g^-$, Figure 4a) and of R_1(CO) = R_2(CO) = 1.30 Å. The results clearly show that the neglect of bending leads to an error in the order of several eV with respect to the energetics of the corresponding excitation energies. Most importantly, however, the omission of the CO_2^+ bending results in a failure to find a covalent structure for the $^4A''$ ($^4B_1$) state of the cation.

Conclusions

The reaction of CO_2^{2+} with neutral CO_2 leads to a $[C_2O_4]^{2+}$ intermediate, which is best described as a complex of the triplet ground state of the dication with the singlet ground state of the neutral reactant. Analysis of the bonding pattern within the $[C_2O_4]^{2+}$ intermediate, by means of the Fermi-hole formalism, shows that the two CO_2 entities are bound via a polar σ-bond between an oxygen atom of originally neutral CO_2 and the carbon atom of CO_2^{2+}. The structural asymmetry of the $[C_2O_4]^{2+}$ intermediate is also associated with an electronic asymmetry: the unpaired electron density stays strictly localized at the O−C−O fragments originating from the doubly charged reactant. The homolysis of the σ-bond between the two $\{CO_2\}$ units thus leads to the formation of the doublet ground state of CO_2^+ from the atoms originating from neutral CO_2 and to the formation of the excited quartet b^4B_2 state of CO_2^+ from the atoms originally belonging to the CO_2^{2+} reactant. This asymmetry can explain the seemingly puzzling "non-statistical" energy distribution in the charge transfer between CO_2^{2+} and CO_2 in a straightforward manner: The $^4B_2$ quartet state correlates with the $CO^+ + O$ dissociation limit and thus explains this fragmentation preferentially observed for the monocation formed by electron capture by the dication. Since similar asymmetries in the energy distributions have also been observed in other systems,[5,10] these results point toward a more important role of transitory intermediates in the electron-transfer reactions of molecular dications with neutral species than previously anticipated. In particular, at low collision energies, the formation of an intermediate in the course of an electron-transfer reaction may play a key role, and therefore these processes cannot always be simply rationalized in terms of "reaction-window theory".[17]

Acknowledgment. This work was supported by the Czech Academy of Sciences (Z40550506), the Grant Agency of the Czech Republic (Grant No. 203/09/1223 (J.R.) and Grant No. 203/118/2009 (R.P.)), the Ministry of Education of the Czech Republic (MSM0021620857, RP MSMT 14/63), and a collaborative grant of the Royal Society London. F.F. thanks the Spanish MICINN for the doctoral fellowship (No. AP2005-2997).

Appendix

Figure 2 shows that, in addition to fundamental splitting of DAFH eigenvectors into two groups, one of which is localized in molecular plane and the other is perpendicular to it, there is also a dramatic difference in the form of the individual eigenvectors associated with α- and β-spin, respectively. Here we show that this surprising difference can straightforwardly be deduced from the interference of the above symmetry based splitting with the isopycnic localization procedure that is the crucial step of DAFH analysis. The key role in this respect belongs to the strict localization of the corresponding eigenvectors in the studied OCO fragment, by which it is possible to deduce the resulting picture of the bonding from the elementary MO description of the topologically equivalent isoelectronic system of the allyl radical (Scheme 4).

SCHEME 4: Schematic Representation of the α- and β-Spin Electrons in the MOs of the Allyl Radical

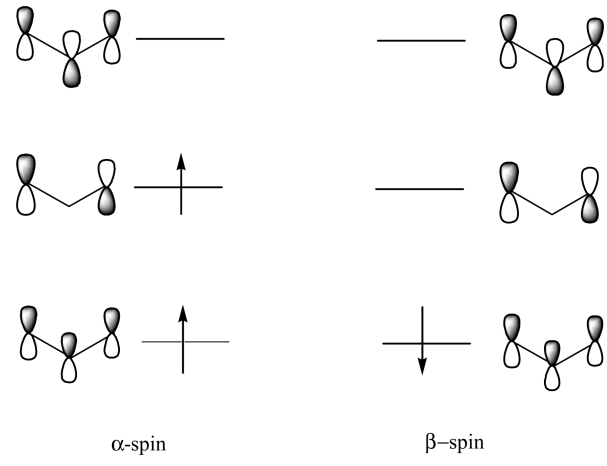

SCHEME 5: Schematic Pair-wise Mixing of α-Spin MOs in the Allyl Radical

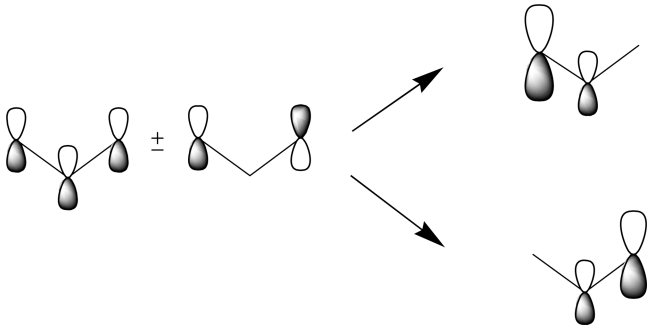

The close parallel of the allyl and OCO systems is immediately suggested by the form of the β-spin DAFH eigenvectors, which exactly mimics the form of the lowest MO of the allyl system. The situation is, however, slightly more complex for the α-spin DAFH eigenvectors, whose form differs from the expectations of the above simple MO scheme. The key to understanding the above difference involves the operation of the isopycnic localization as the crucial step of DAFH analysis. This localization assumes the pair-wise mixing of occupied MOs, and, as it is possible to see from the schematic orbital diagram (Scheme 5), the observed differences in the form of DAFH eigenvectors can be straightforwardly attributed to the possibility and/or impossibility of the mixing for the electrons of α- and β-spin, respectively. This result is very important, since the rationalization of the results of the DAFH analysis in terms of a qualitative MO model reveals sophisticated conclusions concerning the symmetry and multiplicity of the reactive states involved in reaction 1.

References and Notes

(1) Herman, Z. *Phys. Essays* **2000**, *13*, 480.

(2) Herman, Z. *Int. Rev. Phys. Chem.* **1996**, *15*, 299.

(3) Roithová, J.; Žabka, J.; Thissen, R.; Herman, Z. *Phys. Chem. Chem. Phys.* **2003**, *5*, 2988.

(4) Roithová, J.; Herman, Z.; Schröder, D.; Schwarz, H. *Chem.—Eur. J.* **2006**, *12*, 2465.

(5) Roithová, J.; Schröder, D. *Phys. Chem. Chem. Phys.* **2007**, *9*, 731.

(6) Franceschi, P.; Thissen, R.; Žabka, J.; Roithová, J.; Herman, Z.; Dutuit, O. *Int. J. Mass Spectrom.* **2003**, *228*, 507.

(7) Roithová, J.; Ricketts, C. L.; Schröder, D.; Price, S. D. *Angew. Chem., Int. Ed.* **2007**, *46*, 9316.

(8) Ricketts, C. L.; Schröder, D.; Roithová, J.; Schwarz, H.; Thissen, R.; Dutuit, O.; Žabka, J.; Herman, Z.; Price, S. D. *Phys. Chem. Chem. Phys.* **2008**, *10*, 5135.

(9) Žabka, J.; Ricketts, C. L.; Schröder, D.; Roithová, J.; Schwarz, H.; Thissen, R.; Dutuit, O.; Price, S. D.; Herman, Z. *J. Phys. Chem. A*, submitted for publication, 2010.

(10) Parkes, M. A.; Lockyear, J. F.; Price, S. D.; Schröder, D.; Roithova, J.; Herman, Z. *Phys. Chem. Chem. Phys.* **2010**, published online, DOI: 10.1039/b926049h.

(11) Witasse, O.; Dutuit, O.; Lilensten, J.; Thissen, R.; Žabka, J.; Alcaraz, C.; Blelly, P. L.; Bougher, S. W.; Engel, S.; Andersen, L. H.; Seiersen, K. *Geophys. Res. Lett.* **2002**, *29*, 8.

(12) Hogreve, H. *J. Phys. B: At., Mol. Opt. Phys.* **1995**, *28*, L263.

(13) Polak, R.; Hochlaf, M.; Levinas, M.; Chambaud, G.; Rosmus, P. *Spectrochim. Acta A* **1999**, *55*, 447.

(14) Jalbout, A. F. *Int. J. Quantum Chem.* **2002**, *86*, 541.

(15) Hochlaf, M.; Bennett, F. R.; Chambaud, G.; Rosmus, P. *J. Phys. B* **1998**, *31*, 2163.

(16) Schröder, D.; Schalley, C. A.; Harvey, J. N.; Schwarz, H. *Int. J. Mass Spectrom.* **1999**, *185/186/187*, 25.

(17) Roithová, J.; Schwarz, H.; Schröder, D. *Chem.—Eur. J.* **2009**, *15*, 9995.

(18) The ground state of CO_2^{2+} is the major constituent of the CO_2^{2+} dications formed upon CID. See also Mrázek, L.; Žabka, J.; Dolejšek, Z.; Herman, Z. *Collect. Czech. Chem. Commun.* **2003**, *68*, 178.

(19) Ponec, R.; Feixas, F. *J. Phys. Chem. A* **2009**, *113*, 5773.

(20) Žabka, J.; Ricketts, C. L.; Schröder, D.; Roithová, J.; Schwarz, H.; Thissen, R.; Dutuit, O.; Price, S. D.; Herman, Z. *J. Phys. Chem. A*, published online, DOI: 10.1021/jp1023795.

(21) Ponec, R. *J. Math. Chem.* **1997**, *21*, 323.

(22) Ponec, R. *J. Math. Chem.* **1998**, *23*, 85.

(23) Ponec, R.; Duben, A. *J. Comput. Chem.* **1999**, *20*, 760.

(24) Ponec, R.; Roithová, J. *Theor. Chem. Acc.* **2001**, *105*, 383.

(25) Ponec, R.; Cooper, D. L.; Yuzhakov, G. *Theor. Chem. Acc.* **2004**, *112*, 419.

(26) Ponec, R.; Yuzhakov, G.; Carbó-Dorca, R. *J. Comput. Chem.* **2003**, *24*, 1829.

(27) Ponec, R.; Yuzhakov, G.; Gironés, X.; Frenking, G. *Organometallics* **2004**, *23*, 1790.

(28) Ponec, R.; Yuzhakov, G. *Theor. Chem. Acc.* **2007**, *118*, 791.

(29) Bader, R. F. W. *Atoms in Molecules. A Quantum Theory*; Clarendon Press: Oxford, 1994.

(30) Cioslowski, J. *Int. J. Quantum Chem.* **1990**, *S24*, 15.

(31) Ponec, R.; Cooper, D. L. *Faraday Discuss.* **2007**, *135*, 31.

(32) Frisch, M. J.; Trucks, G. W.; Schlegel, H. B.; Scuseria, G. E.; Robb, M. A.; Cheeseman, J. R.; Montgomery, J. A., Jr.; Vreven, T.; Kudin, K. N.; Burant, J. C.; Millam, J. M.; Iyengar, S. S.; Tomasi, J.; Barone, V.; Mennucci, B.; Cossi, M.; Scalmani, G.; Rega, N.; Petersson, G. A.; Nakatsuji, H.; Hada, M.; Ehara, M.; Toyota, K.; Fukuda, R.; Hasegawa, J.; Ishida, M.; Nakajima, T.; Honda, Y.; Kitao, O.; Nakai, H.; Klene, M.; Li, X.; Knox, J. E.; Hratchian, H. P.; Cross, J. B.; Bakken, V.; Adamo, C.; Jaramillo, J.; Gomperts, R.; Stratmann, R. E.; Yazyev, O.; Austin, A. J.; Cammi, R.; Pomelli, C.; Ochterski, J. W.; Ayala, P. Y.; Morokuma, K.; Voth, G. A.; Salvador, P.; Dannenberg, J. J.; Zakrzewski, V. G.; Dapprich, S.; Daniels, A. D.; Strain, M. C.; Farkas, O.; Malick, D. K.; Rabuck, A. D.; Raghavachari, K.; Foresman, J. B.; Ortiz, J. V.; Cui, Q.; Baboul, A. G.; Clifford, S.; Cioslowski, J.; Stefanov, B. B.; Liu, G.; Liashenko, A.; Piskorz, P.; Komaromi, I.; Martin, R. L.; Fox, D. J.; Keith, T.; Al-Laham, M. A.; Peng, C. Y.; Nanayakkara, A.; Challacombe, M.; Gill, P. M. W.; Johnson, B.; Chen, W.; Wong, M. W.; Gonzalez, C.; Pople, J. A. *Gaussian 03*, revision C.02; Gaussian, Inc.: Wallingford, CT, 2004.

(33) Keith, T. A. *Program AIMAll*, 1997−2010 (aim.tkgristmill.com).

(34) Èížek, J. *Adv. Chem. Phys.* **1969**, *14*, 35.

(35) Dunning, T. H., Jr. *J. Chem. Phys.* **1989**, *90*, 1007.

(36) Knowles, P. J.; Werner, H.-J. *Chem. Phys. Lett.* **1985**, *115*, 259.

(37) Werner, H.-J.; Knowles, P. J. *J. Chem. Phys.* **1988**, *89*, 5803.

(38) Knowles, P. J.; Werner, H.-J. *Chem. Phys. Lett.* **1988**, *145*, 514.

(39) MOLPRO 2006.1 is a package of ab initio programs written by Werner, H.-J.; Knowles, P. J. with contributions from Amos, R. D.; Bernhardsson, A.; Berning, A.; Celani, P.; Cooper, D. L.; Deegan, M. J. O.; Dobbyn, A. J.; Eckert, F.; Hampel, C.; Hetzer, G.; Korona, T.; Lindh, R.; Lloyd, A. W.; McNicholas, S. J.; Manby, F. R.; Meyer, W.; Mura, M. E.; Nicklass; Palmieri, P.; Pitzer, R.; Rauhut, G.; Schütz, M.; Stoll, H.; Stone, A. J.; Tarroni, R.; Thorsteinsson, T. See http://www/molpro.net.

(40) Liu, J. B.; Chen, W. W.; Hochlaf, M.; Qian, X. M.; Chang, C.; Ng, C. Y. *J. Chem. Phys.* **2003**, *118*, 149.

JP1020559